SUNTEXT REVIEWS

SunText Review of Medical & Clinical Research
ISSN: 2766-4813

Open Access
Original Article
Volume 2:4

Analysis for Brain Tumors and Alzheimer's Disease Using Quantum Microrna Language with Artificial Intelligence (MIRAI)

Yoichi Robertus Fujii*

Kawada-Cho, 106-6, Atsuta-Ku, Nagoya, 456-0065, Japan

***Corresponding author:** Yoichi Robertus Fujii, Kawada-Cho, 106-6, Atsuta-Ku, Nagoya, 456-0065, Japan; Tel: +81-52-682-7003; E-mail: fatfuji@hotmail.co.jp

Received date: 26 November 2021; **Accepted date:** 30 November 2021; **Published date:** 04 December 2021

Citation: Robertus Fujii Y (2021). Analysis for Brain Tumors and Alzheimer's Disease Using Quantum Microrna Language with Artificial Intelligence (MIRAI). SunText Rev Med Clin Res 2(4): 142.

DOI: https://doi.org/10.51737/2766-4813.2021.042

Abstract

Background: Alteration in plasma/serum microRNA (miRNAs) profiles are associated with brain cancer and Alzheimer's disease (AD). Circulating miRNA profiles could be the first choice of non-invasive biomarker candidates for the prediction, diagnosis and prognosis of human disease. To further investigate the function of circulating miRNAs in brain tumors and AD to build sustainable healthcare, in silico analysis was performed using a quantum miRNA language with artificial intelligence (MIRAI) with miRNA diagnostic panels.

Methods: Data from serum/plasma miRNA panels from patients with AD or brain cancer was extracted from the database. The miRNA memory package (MMP) from the miRNA diagnostic panel were selected by data mining. The miRNA entangling target sorter (METS) bioinformatics algorithm using MIRAI was used to analyze the etiology according to the procedure previously described.

Result: Hub miRNA/targeting protein links on glioma and astrocytoma data were extracted as upregulation of high mobility group AT-hook 1 (HMGA1) by miR-16-5p (down regulation) and up regulation of BCL2 apoptosis regulator (BCL2) by miR-497-5p (down regulation), and down regulation of RB transcriptional coreceptor 1 (RB1) by miR-106a-5p (up regulation) and down regulation of cyclin dependent kinase inhibitor 1A (CDKN1A) by miR-20a-5p (up regulation), respectively. AD was associated with circadian rhythm, ribosomopathy and the vascular endothelial growth factor A (VEGFA) signalling pathway. Enhanced VEGFA expression through down regulation of miR-361-5p was a vivid cause of AD. Elevation of the circadian rhythm-related protein, aryl hydrocarbon receptor nuclear trans locator like (ARNTL) via down regulation of miR-142-3p was the underlying pathogenicity of mild cognitive impairment (MCI) and AD; therefore, no inverse correlation between common miRNA hubs and hub miRNA levels was observed between AD and brain cancers.

Conclusion: Given the hub miRNAs in brain cancer and AD, there were no common miRNAs from MMPs among disease. Thus, miRNA biomarkers for brain cancer, MCI and AD could be available for pathophysiologic diagnosis and prediction. It is the first in silico report that high levels of VEGFA due to down regulation of miR-361-5p may be a cause of progression from MCI to AD via angiodysplasia. As miR-361-3p and -5p were targeted to the BACE1 3'UTR, anti-VEGFA agent and/or miR-361 stem loop mimicking locked nucleic acid (LNA) treatment may be effective approaches to MCI or early AD prevention.

Keywords: microRNA; Aging; Quantum; Alzheimer; Glioma; Network; Astrocytoma

Introduction

Gliomas are the most prevalent malignant tumor in brain cancers, accounting for 81%. The incidence of glioma in adults is rare, approximate 0.1 to 0.5 in million people [1]. From World Health Organization (WHO) classification of tumors of the central nervous system, gliomas histologically contain the most common glioblastoma and astrocytoma in diffuse astrocytic and oligodendroglial tumors. However, there is no consensus definition of gliomas as a larger class of histology [2]. For example, gliomas are classified from grade I to IV by WHO

according to malignant behavior; however, in the class of diffuse astrocytic and oligodendroglial tumors, diffuse astrocytoma on isocitrate dehydrogenase gene (IDH)-mutant is the WHO grade II tumor, and glioblastomas on IDH wild type and IDH-mutant are the WHO grade IV tumor. The 5-year relative survival rate for glioma is only 0.1-5% [1]. Temozolomide (TMZ) is a standard chemotherapeutic agent that targets gliomas, and acts by methylation and crosslinking of DNA in glioma cells [3]. Surgery followed by concurrent radiotherapy plus TMZ chemotherapy is recommended as current protocolized treatments for high-grade glioma [4]. It is estimated that approximately 36 million people worldwide would suffer from Alzheimer's disease (AD) and other dementias in 2010, and the number of AD is predicted to grow rapidly. For example, there will be 66 million in 2030 and 115 million in 2050 [5]. There are two types of dementia. The first is AD. AD is characterized by a progressive, unremitting and neurodegenerative disorder. The other is vascular cognitive impairment and dementia (VCID). VCID is caused by hypertension and arteriosclerosis, including amyloid angiopathy, infraction and ischemic attacks to induce cerebrovascular damage [6]. VCID comprises mild cognitive impairment (MCI), vascular dementia (VaD), and mixed vascular and AD-type cognitive impairment [7]. Although AD is the most common type of dementia, AD is complex and has been diagnosed by the mini-mental state examination (MMSE), neuropsycological tests, magnetic resonance imaging (MRI), positron emission tomography (PET) and the single-photon emission computed tomography (SPECT) with machine learning [8]. While the effective diagnosis of AD, its prodromal stage-MCI including amnestic MCI (aMCI) and nonamnestic MCI (naMCI) have recently been performed by machine learning on MRI plus MMSE, the protocol provided an average accuracy of 92.4%, sensitivity of 84% and specificity 96.1% for MCI versus cognitively normal (CN). However, it is mathematically calculated that the USA model requires approximate $8 trillion in medical and care cost to diagnose AD early and accurately [9,10]. Therefore, for establishing sustainable health management, less expensive and simpler diagnostic tools should need to be developed for the initial diagnosis of AD and MCI in the early stage. It is well known that amyloid β (Aβ), tau and apolipoprotein E (APOE) are the major elements contributors to AD. Senile plaques are consisted by Aβ, and amyloidopathy of the cerebrovasculature, and loss of neurons in the temporal lobes were pathologically observed in AD [11]. Aβ is produced from amyloid β precursor protein (APP) digested by β-secretase 1 (BACE1) [12]. Progressive tau accumulation has been found in the medial and lateral temporal cortices of APOE ε4 genotype AD patients in a PET study [13]. Although the APOE ε4 allele status was significantly correlated with the level of tau neurofibrillary tangle, the pathology of tau was independent of Aβ plaques in PET clinical analysis [14]. Plasma analysis showed that Aβ+ participants had a significantly higher proportions of APOE ε4 genotype carriers than Aβ- in MCI [15]. Except for hereditary AD, most AD patients are sporadic; however, APOE ε4 genotype is involved in Aβ/tau accumulation in different states of neurodegeneration and in different sample sources. On the clinical side, the effective reduction of plaques or plasma Aβ by numerous drug candidates for AD might have not provided clinical benefit, as well as the approval of aducanumab by the U. S. Food and Drug Administration (FDA) in June 7th, 2021 could be; therefore, the fundamental question remains that Aβ and tau might be 'results' of AD but not their 'causes' [16-20]. On the contrary, ribosomal deficiencies, such as the ribosomopathy have been observed in early AD and MCI [21,22]. Therefore, impaired ribosome biogenesis and protein synthesis would be characteristic of MCI. Further, since vascular endothelial growth factor A (VEGFA) secretion from astrocytes has been increased by Aβ42, VEGF is also implicated in AD. High levels of VEGF resulted in loss of insoluble Aβ42 and increasing of blood-brain barrier (BBB) permeability [23-26]. Conversely, the soluble form of the VEGF receptor (sVEGFR) was reduced in the plasma of AD compared to healthy control subjects [27]. These results suggest that sVEGFR is an antagonist of VEGFRs, VEGFR-1 (FLT1) and -2 (KDR) during the angiogenic process, and by its decreasing, VEGF may protectively affect human vascular endothelial cells to remove insoluble Aβ. But high levels of VEGFA may inversely increase soluble Aβ. Subsequently, despite of these VEGF effects, the mechanisms by which the clinical status of MCI progresses remains unclear. We have previously investigated common neurodegeneration susceptible universal microRNAs (miRNAs) by in silico simulation of miRNA entangling target sorting (METS) among 105 miRNAs in Alzheimer's disease, 44 miRNAs in Parkinson's disease, 28 miRNAs in frontotemporal dementia, and 93 miRNAs in Huntington's disease [28]. Seven miRNAs, miR-34b/c, miR-29a-3p, miR-29b-3p, miR-124-3p, miR-9-3p, miR-132-3p and miR-138-5p were common, and was thought to be involved in the memory mechanism of the brain. Seven protein targets, Notch receptor 1 (NOTCH1), Sirtuin 1 (SIRT1), histone deacetylase 4 (HDAC4), methyl-CpG binding protein 2 (MeCP2), brain derived neurotrophic factor (BDNF), BACE1 and α-amino-3-hydroxy-5-methyl-4-isoxazolepropionic acid receptor (AMPAR) were extracted by computer analysis and linked to the above 7 miRNAs and 7 proteins in the network. Our data has been corroborated by a previous report that three miRNA panel of miR-132, miR-124 and miR-34 are associated with memory impairment [29]. Meanwhile, in another repots, miR-30b-5p has been overlapped among Alzheimer's disease, Parkinson's disease, multiple sclerosis and amyotrophic lateral sclerosis [30]. However, it remains unclear whether the functional universal miRNA panel can distinguish between age-related cases of

Alzheimer's disease and human neurodegenerative disorders and human brain tumor. In addition, by γ-secretase substrate presenilin gene (PSEN) double-knockout mouse of a model for human AD, increasing of tumor suppressor miRNAs has been observed, and a negative correlation between AD and cancer was showed [31]. But clinical analysis in humans has less been reported much comparison between miRNA-based AD and cancer etiologies [32,33]. Definitive diagnosis of AD is challenging, and the etiology analysis of AD with diagnosis would be the most difficult goal in neurology. It has been reported as diagnostic markers for dementia to detect miRNAs, interleukin-10 (IL-10), IL-6 in the plasma/serum and Aβ, tau in cerebrospinal fluid (CSF); however, their effectiveness and clinical discrimination among other inflammation diseases have been disputed points except for miRNA biomarkers [11, 34-37]. Therefore, miRNA non-invasive biomarker in the circulating system would be useful for early diagnosis of dementia including diagnosis of the presence or absence of cognitive impairment such as AD and MCI. We have reported that the etiology of viral infection can be simulated in miRNA biomarker panels by using the quantum miRNA language plus artificial intelligence (MIRAI), such as hepatitis B virus (HBV), hepatitis C virus (HCV) and human immunodeficiency virus (HIV-1) [38]. Circulating miRNA biomarkers have also revealed the pathogenic mechanisms of human cancer, breast, lung, colorectal, pancreatic, esophageal, gastric cancers and liver cancers, which is in good agreement with the National Institute of Health (NIH) definition of biomarkers. The etiology of severe acute respiratory syndrome human coronavirus 2 (SARS-Cov-2) has not yet been known clearly, but we have firstly revealed in silico the etiology of coronavirus disease 2019 (COVID-19) from miRNA profiles of SARS-CoV-2 infection [39-44]. In addition, by using the same algorithm as MIRAI above, we discovered that rice MIR2097-5p could act as anti-COVID-19 therapeutic miRNA agents. Furthermore, it has been shown that COVID-19 vaccine (BNT162b2) has potency of a miRNA vaccine [45,46]. Thus, miRNAs have been investigated as candidates for non-invasive AD biomarker, where we simulated neurodegeneration etiology with a quantum miRNA language with MIRAI using miRNA biomarker panels from serum or plasma. Circulating miRNA data in brain cancers and AD were useful to elucidate their etiology. Particularly, in the analysis of MCI, computer simulations provided predictive results that could distinguish the etiology of MCI and AD. Consequently, it was showed that activation of the VEGF signaling pathway regulated by miRNAs is a major cause of AD [47]. Then, therapeutic miRNA agents were discussed.

Materials and Methods

Database usage

Google Scholar (https://scholar.google.co.jp) was firstly used for data extraction from miRNA panels and miRNA profiles in plasma or serum. PubMed (pubmed.ncbi.nim.nih.gov), in which our treatise data is not listed and not affected to AI analysis as a false premise bias, was also used. Total information content was 502,268 in aging, 216,289 in brain cancer, 103,170 in glioma and 44,434 in astrocytoma, 81,297 in neurodegeneration, and 165,704 in AD. Gene functions of protein and RNA genes were searched by GeneCards (www.genecards.org). Protein ontology was investigated by GO enrichment analysis in Geneontology (geneontology.org).

METS analysis

METS analysis was performed by a computer processing algorithm as described previously [48]. Shortly, miRNA memory package (MMP) was extracted from miRNA biomarker panels and profiles. Data mining about miRNA panels and profiles for the standard setup of MMPs was performed by: 1) data from serum or plasma, 2) cleared in expression levels of up- and down-regulation, 3) data was statistically analyzed by receiver operating characteristic (ROC) and the cut off value of an area under the curve (AUC) about biomarker profiling is 0.8. As quantum miRNA language, single miRNA quantum energy level in an MMP was calculated as single nexus score (SNS) (Table 1).

Table 1: *MMPs in brain cancers and AD.*

AD and tumor	Data source	AUC data	miRNA	Level	SNS	Source	Reference No.
Brain cancer	Glioma	>0.75	**miR-497-5p**	down	6	serum	51-53
			miR-125b-5p	down	4	serum	
			miR-16-5p	down	6	plasma	
			miR-21-5p	up	5	serum	
			miR-222-5p	up	5	serum	
			miR-124-3p.1	up	7	serum	
	Astrocytoma	0.9722 in a panel	miR-15b-5p	up	4	serum	59
			miR-16-5p	up	6	serum	

			miR-19a-3p	up	4	serum	
			miR-19b-3p	up	4	serum	
			miR-20a-5p	up	7	serum	
			miR-106a-5p	up	7	serum	
			miR-130a-3p	up	6	serum	
			miR-181b-5p	up	7	serum	
			miR-208a-3p	up	5	serum	
AD	MCI panel	>0.9	**miR-483-5p**	up	11	plasma	62
			miR-486-5p	up	6	plasma	
			miR-30b-5p	down	2	plasma	
			miR-200a-3p	up	5	plasma	
			miR-502-3p	up	6	plasma	
			miR-142-3p.1	down	5	plasma	
	US & Germany cohorts	>0.8	miR-17-3p	up	7	plasma	63
			miR-5010-3p	down	3	plasma	
			let-7d-3p	down	3	plasma	
			miR-26b-5p	up	5	plasma	
			miR-28-3p	down	6	plasma	
			miR-361-5p	down	5	plasma	
			miR-532-5p	up	7	plasma	
	Conventional, Meta-analysis	>0.876	**miR-34a-5p**	up	8	plasma	64-66
			miR-34c-5p	up	8	plasma	
			miR-7-5p	down	7	plasma	
			miR-191-5p	down	5	plasma	
			let-7g-5p	down	7	plasma	
			miR-15b-5p	down	4	plasma	
			miR-142-3p.1	down	5	plasma	

Bold: hub miRNAs

Next, entangling double miRNAs' quantum energy levels as double nexus score (DNS) were computed by multiplication of two SNSs in a matrix based on the scalar product with electron spin [28]. To apply quantum miRNA language to the METS algorithm, DNS data of multi-targets to a miRNA and multi-miRNAs to a target in the higher dimension matrix was computed from data of Target Scan Human 7.2, DIANA-TarBase and miRTarBase Ver. 8.0 or mirtarbase data for miRTarBase release 6.1, which was re-built up by Excel file of packages in the GitHub . The valid DNS values of miRNA/target connections were determined by the optional cut-off value. Protein/protein interaction search and cluster analysis were performed by using STRING Ver. 11.0. Network among miRNAs and target proteins was constructed from the METS algorithm according to data from MIRAI.

METS analysis with MIRAI

MIRAI was used for validation for METS and extraction of hub miRNAs. An AUC in ROC, accuracy, and precision was calculated as previously described [44]. Previous METS analysis data in pancreatic, lung, colorectal, gastric, esophageal and liver cancers was combined with present data of METS analysis in AD and brain cancers.

Results and Discussion

Distribution of quantum energy in brain cancers and AD

MMPs were extracted from circulating miRNA panels. MiRNA/miRNA mutual (DNS) quantum energy frequencies in each layer used in METS algorithms, named the Quantum Core Region (QCR), were computed. Frequency of quantum energies in MCI (AD MCI), AD on USA & Germany cohorts (AD USA & Germany) and on conventional AD miRNA panel in meta-analysis (AD Conventional), gliomas and astrocytoma. QCR of hub miRNAs in AD and glioma was at 21-40 QRC (brown bars), which was in a peak quantum energy frequency layer. Profile of miRNAs in AD is completely different between conventional panel and USA & Germany panel, and conventional AD panel differed from USA & German panel in that it contains a high

quantum energy frequency 61-80 QCR region. On the other hand, QCR regions of brain cancers were similar in each other. USA & Germany AD hub miRNAs and conventional AD hub miRNAs were located at 21-40 QCRs (orange arrows). Glioma miRNA hub was also on the 21-40 QCR (orange arrow). MCI and astrocytoma miRNA hubs were in 41-60 QRCs (gray arrows). Data clearly suggests that quantum energy levels in brain disease are moderate. MiRNA QCR layers were cohered for METS analysis and network among miRNAs and protein/protein cluster was calculated from the data (Figure 1).

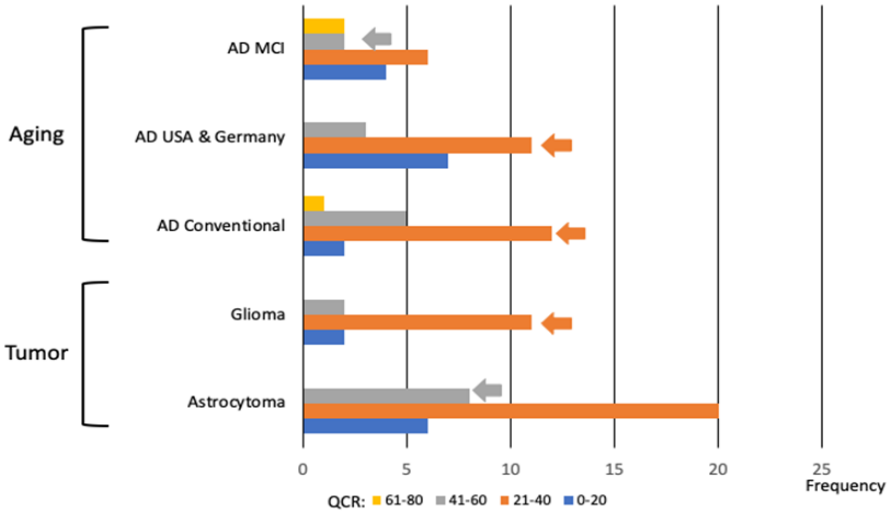

Figure 1: *The quantum energy levels of miRNA in aging and tumor in the brain. DNSs between two miRNAs in MMP were computed.*

Brain tumour

Recently, a set of miRNAs de-regulation between the brain tumor and AD has been identified, and it has been demonstrated that the levels of tissue expression in the set of miRNAs are inversely associated between the tumor and AD [32]. Further, circulating miRNAs overlapped between cancer and AD has been found and their expression levels were usually opposite [33]. Therefore, METS analysis of brain cancer was performed to confirm the inverse relationship between cancer and AD miRNA expression, and as a data size control, including single panel or mixed panels, of MIRAI in AD and MCI pathophysiological changes.

Glioma and astrocytoma

Circulating microRNAs have been identified as a biomarker of glioma [49,50]. In our simulation, the MMP of glioma (WHO grade II/III and IV) was selected from three circulating miRNA panels according to the data mining rules. It contained six miRNAs, miR-497-5p, miR-125b-5p, miR-16-5p, miR-21-5p, miR-222-5p and miR-124-3p.1 [51-53]. MiR-497-5p, miR-125b-5p and miR-16-5p have been down regulated, and miR-21-5p, miR-222-5p and miR-124-3p.1 were up regulated (Figure 2).

Targets of miR-125b-5p had no linkage of protein/protein cluster and targets of miR-21-5p were not computed by below cut-off DNS value in METS data (data not shown). Hub miRNAs were miR-16-5p and miR-497-5p in pathogenic analysis of glioma. About targets of the miRNA, HMGA1 and BCL2 were up regulated by decreasing of miR-16-5p hub with let-7b-5p, let-7a-5p and miR-196a-5p, and with miR-34a-5p. BCL2 was also enhanced by down regulation of miR-497-5p with miR-34a-5p. HMGA1 expression has been observed in 96.7% of malignant glioma (WHO grade II/III) but not in normal brain tissues, and the expression of HMGA1 in human glioma significantly correlated with VEGFA expression [54]. MiR-361-5p was downregulated in glioma tissues and was inversely correlated with glioma grade [55]. Hence, the relation between VEGFA and miR-361-5p in glioma tissues may be analogous to that in AD. But there is no paper about miR-361-5p as a circulating miRNA marker of glioma. MiR-16-5p expression in glioma has been lower than non-cancerous brain tissues and upregulation of miR-16-5p promoted apoptosis via suppression of BCL2 [56].

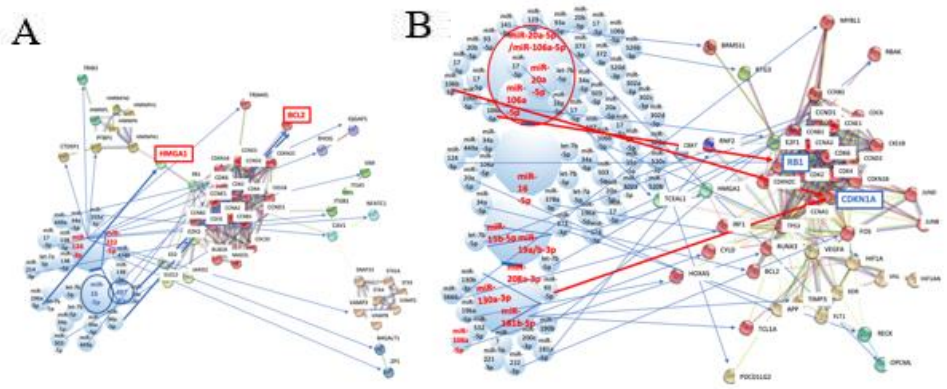

Figure 2: *The network scheme of METS simulation in a miRNA biomarker panel of glioma and astrocytoma. Linkages among protein clusters and miRNA/miRNA were depicted by METS algorithm in glioma (A) and astrocytoma (B). miRNAs in red: upregulation, proteins in blue: downregulation. Red circle is the hub miRNAs. Small circles in blue are the hub miRNAs.*

B flavone agent, apigenin has induced apoptosis of U87 human glioma cells via increasing of miR-16-5p and suppression of BCL2 [57]. Further, breast cancer cell apoptosis has been induced by up regulation of miR-497-5p through negative regulation of BCL2 [58]. An AUC of glioma with MIRAI was 1.00 (accuracy, 1.00; precision, 1.00; recall, 1.00; F value, 1.00). Thus, it was found that the key protein targets are HMGA1 and BCL2 in glioma. As BCL2 was down regulated in AD, the levels of BCL2 expression was inverse between AD and glioma; however, effector miRNAs were different in two brain diseases. The MMP of astrocytoma was determined. Nine miRNAs, miR-15b-5p, miR-16-5p, miR-19a/b-3p, miR-20a-5p, miR-106a-5p, miR-130a-3p, miR-181b-5p and miR-208a-3p were selected from a miRNA panel of serum from patients with astrocytoma (WHO grade II, 30%; III 40%; IV, 30%) [59]. All miRNAs have been up regulated. The hub miRNA was miR-106a-5p or miR-20b-5p in the etiologic analysis of astrocytoma. RB1 was blocked by up regulation of miR-106a-5p in combination with miR-106b-5p. Cyclin dependent kinase inhibitor 1A (CDKN1A) was inhibited by up regulation of miR-20a-5p and miR-106a-5p along with miR-93-5p, miR-20b-5p, miR-17-5p and miR-106b-5p, and up regulation of miR-208-3p with miR-93-5p. Since tumor suppressor proteins, RB1 and CDKN1A were down regulated, up regulation of miR-106a/b-5p and miR-20a-5p would be carcinogenic in the brain. Although miR-106a/b-5p and miR-20a-5p have been up regulated in pediatric medullblastoma (WHO grade IV), ependymoma (grade II) and pilocytic astrocytoma (grade I) tissues, there was no other reports about the circulating miR-106a/b-5p and miR-20a-5p profiles in patients with astrocytoma (grade II-IV) [60]. In glioblastoma CD133+ stem cell lines, miR-106a-5p and miR-20a have been enhanced [61]. An AUC of astrocytoma with MIRAI was 0.99 (accuracy, 0.96; precision, 0.98; recall, 0.98; F value, 0.98). Since data of therapeutic targets was statistically significant, we found two key protein targets, RB1 and CDKN1A on astrocytoma.

MMPs for the etiological analysis in MCI and AD

Three MMPs of miRNAs in AD computer simulation were prepared from circulating miRNA biomarker in plasma. MMP of MCI contains six miRNAs of miR-483-5p, miR-486-5p, miR-30b-5p, miR-200a-3p, miR-502-3p and miR-142-3p.1 from a panel (AUC >0.9) (Mini-Mental State Examination, MMSE: 25.9 in MCI; 20.4 in AD) [62]. MiR-483-5p, miR-486-5p, miR-200a-3p and miR-502-3p have been up regulated, and miR-30b-5p and miR-142-3p.1 were down regulated. In the case of AD on USA & Germany cohort data (MMSE: 20.0 in AD; 29.1 in healthy control), seven miRNAs, miR-17-3p, miR-5010-3p, let-7d-3p, miR-26b-5p, miR-28-3p, miR-361-5p and miR-532-5p were prepared as MMP (AUC >0.8) [62,63]. MiR-17-3p, miR-26b-5p and miR-532-5p have been up regulated, and miR-5010-3p, let-7d-3p, miR-28-3p and miR-361-5p were down regulated. A panel of conventional case from data of meta-analysis (AUC >0.876) contained seven miRNAs of MMP, miR-34a-5p, miR-34c-5p, miR-7-5p, miR-191-5p, let-7g-5p, miR-15b-5p and miR-142-3p.1 [64-66]. MiR-34a/c-5p has been up regulated and 5 miRNAs remained were down regulated. There was no linkage of protein/protein cluster to miR-30b-5p and miR-502-3p in MCI data, miR-28-3p and 361-5p in USA & Germany cohort data, and miR-191-5p and miR-15b-5p in conventional meta-analysis data (data not shown). Targets against let-7-3p and miR-5010-3p in USA & Germany were not computed by below the cut-off DNS value in METS data (data not shown).

Ribosomopathy and circadian rhythm dysregulation upon MCI

About target proteins against circulating biomarker miRNAs of MCI, have determined that the center of network is the mitochondrial respiratory chain pathway involving in oxidative stress [62]. When our METS analysis was performed by MCI microRNA data, ribosomal protein L31 (RPL31) was suppressed by upregulation of miR-483-5p along with miR-409-5p and miR-653-5p (Figure 3).

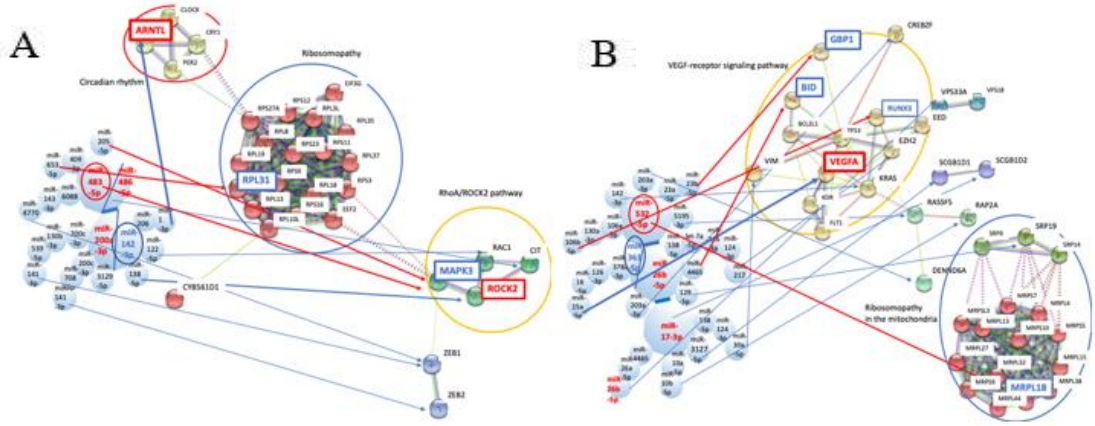

Figure 3: *Network diagram of METS simulation in a biomarker panel of the MCI stage and AD USA & Germany cohorts. Interaction among protein and miRNA/miRNA was simulated by METS analysis in MCI (A) and AD (B). miRNAs and proteins in red: upregulation, in blue: downregulation. Small circles in red and blue are the hub miRNAs. Large circles in red (circadian rhythm), in blue (ribosomopathy or ribosomopathy in the mitochondria) and in yellow (VEGF-receptor signaling pathway) are presented as GO functions.*

RPL31 is a component of the 60S RNA subunit with ribosomal protein. Decreasing of protein synthesis via impairment of ribosomal function has been found in MCI and expression of RPL31 has been reduced in AD, which is a ribosomopathy [67,68]. While we have previously shown that human ribosomal RNA derived miRNAs would be implicated in carcinogenesis as a ribosomopathy, and ribosomopathies lead to oxidative stress via the mitochondria, present data and suggests that ribosomal malfunction by upregulation of miR-483-5p would induce the stress against neural cells. It is well known that disturbed circadian rhythms with sleep problem is implicated in AD, and circadian locomotor output cycles gone kaput (CLOCK) gene and external Zeitgeber are related with circadian rhythmicity [69-71]. Disturbance of circadian rhythm occurs in an early AD as well [72]. However, molecular targets of circadian rhythmicity for early AD therapeutic inventions have not yet been provided. In our simulation, expression of aryl hydrocarbon receptor nuclear translocator like (ARNTL, BMAL1) was augmented by downregulation of miR-142-3p in combination with miR-206 and miR-1-3p. ARNTL is a core component of the circadian clock, which forms a heterodimer with clock circadian regulator (CLOCK). Although in AD mouse model experiments, loss of ARNTL in the brain parenchyma increased expression of APOE and Aβ accumulation, protein expression levels of human ARNTL and CLOCK have significantly elevated in impaired astrocytes of cerebral cortex from patients with AD [73,74]. Therefore, enhancement of ARNTL and CLOCK may promote apoptotic cytotoxicity via metabolic dysfunction in human astrocytes. Imaging analysis by fluorodeoxyglucose (FDG)-positron emission tomography (PET) have showed hypometabolism and reducing utilization of glucose in the brain with AD [75]. These results strongly support that aberration of circadian rhythm would be associated with neurodegeneration, and downregulation of miR-142-3p participated in mechanisms of MCI [76,77]. Citron Rho-interacting serine/threonine kinase (CIT) and mitogen-activated kinase 3 (MAPK3) were inhibited by upregulation of miR-486-5p and upregulation of miR-483-5p with miR-205-5p. MAPK overlaps in a report [62]. Further, Rac family small GTPase 1 (RAC1) and Rho associated coiled-coil containing protein kinase 2 (ROCK2) were increased by downregulation of miR-142-3p with miR-122-5p and with miR-138-5p, respectively. From GO analysis, these four proteins in a cluster were dominantly implicated in RhoA/ROCK2 pathway (GO: 0007266), which was also related with upstream VEGF receptor (GO: 0005021). VEGF signaling pathways is the major process of angiogenesis and vasculogenesis, and ROCK 1 and 2 inhibition has activated angiogenesis via VEGFA/Ras homolog family member A (RhoA) [78]. Therefore, inhibition of VEGF/VEGFR/RhoA/ROCK/mitogen-activated kinase (MAPK) axis may progress MCI condition. However, VEGF/VEGFR-1 or VEGF/VEGFR-2 signaling directly or indirectly can transduce to angiogenesis without affecting through the RhoA/ROCK/MAPK pathways because RhoA controls diverse pathways, such as RhoA/actin-regulating kinase PRK1 (PRK1) /

phosphatidylinositol-4-phosphate5-kinase (PIP5K)/phospholipase D (PLD) pathway [79]. These data suggest that suppression of MAPK3 and augment of ROCK2 may partly be anti-angiogenesis effects via VEGF signalling pathway. But the altered expression of VEGF has not been observed in MCI [79]. Finally, by MIRAI, it was resulted that an AUC about the etiology of MCI in AD subjects was 0.53 (accuracy, 0.86; precision, 0.92; recall, 0.92; F value, 0.95), in contrast, an AUC of a diagnostic miRNA panel in MCI has been over 0.9 as described above. It is showed that the miRNA panel is useful for differential diagnosis to distinguish MCI in neurodegenerative disease in precious medicine. Further, another plasma miRNA biomarker panel and validation study have been documented in MCI [80]. Six miRNA biomarkers, miR-132-3p, miR-128-3p, miR-874-3p, miR-134-5p, miR-382-5p and miR-323b-5p (AUC, >0.9) have been up regulated in plasma of patients with MCI. The etiologcal analysis of this panel was performed according to the METS simulation with MIRAI procedures (data not shown). Although GO analysis of miRNA-target proteins showed just the cell cycle-related protein cluster alone (GO: 0061575), an AUC about the etiology in AD was 0.64 (accuracy, 0.80; precision, 0.94; recall, 0.85; F value, 0.89). The results of validation data were similar pattern to data [62]. Cell cycle dysregulation may not dominantly be the primary cause of MCI. If in MCI the validated results of circulating miRNA biomarker were distinct from those as AD of the etiology analysis as below, diagnostic miRNA biomarker would be available for precious medicine of neurodegeneration.

VEGF signaling, ribosomopathy and circadian rhythm dysregulation upon AD

AD USA & Germany panel have already extracted a GO enrichment analytic data from the miRTarBase, which included ATP binding cassette subfamily A member 1 (ABCA1), Death associated protein kinase 1 (DAPK1), Insulin-like growth factor 1 receptor (IGF1R) and VEGFA in aging, and cyclin D1 (CCND1), cyclin E1 (CCNE1), cyclin E2 (CCNE2), cyclin dependent kinase 6 (CDK6), MYC proto-oncogene (MYC), RAD51 recombinase (RAD51) and RB transcriptional corepressor 1 (RB1) in DNA damage response; however, they were unable to exclude some biases about selection of miRNA small sets and targets. Whereas, in our METS analysis, VEGFA was upregulated by downregulation of miR-361-5p along with miR-378a-3p, miR-126-3p, miR-16-5p and miR-15a-5p. Further, enhancer of guanylate binding protein 1 (GBP1) was blocked by upregulation of miR-532-5p with miR-23a/b-5p. Human GBP1 has reduced VEGF expression in mouse cancer model [81]. Therefore, reduction of GBP1 may contribute VEGFA secretion. VEGFA secretion from astrocytes is increased by Aβ42; therefore, VEGFA increasing would be deeply implicated in AD as described above. Further, VEGF genotypes or haplotypes was not associated with AD in the case-control study, suggesting that high levels of VEGFA by downregulation of miR-361-5p may be the major cause of AD, which is acquired but not be genetical. BH3 interacting domain death agonist (BID) was suppressed by upregulation of miR-26b-5p with miR-4465. BID is a death agonist and antagonist of BCL2 apoptosis regulator (BCL2), and BID is a mediator of mitochondrial damage by caspase-8; therefore, BID is proapoptotic protein [82,83]. Since myeloid cell leukemia-1 (MCL-1) was induced by VEGF and MCL-1 inhibited cell apoptosis by BCL2 associated X (BAX), the VEGF/MCL-1/BAX axis was associated with prostate cancer metastasis. Accordingly, BID suppression and VEGF upregulation may be implicated in anti-apoptotic and indirectly migrating effects to Aβ accumulated neural cells. RUNX family transcription factor 3 (RUNX3) was inhibited by upregulation of miR-532-3p with miR-106a/b-5p and miR-130a-3p. RUNX3 knockdown has enhanced endothelial progenitor cell function through VEGF/MAPK/AKT serine-threonine kinase (AKT) pathway [84]. Therefore, decline of RUNX3 may induce excessive angiogenesis. From GO analysis, these four proteins in a cluster were implicated in VEGFR signaling pathway (GO: 0048010). Altogether, it is suggested that VEGFA-autocrine/paracrine would be increased by Aβ accumulation and it may induce to inhibit apoptosis of Aβ accumulated neural cells. White matter hyperintensities (WMH) in magnetic resonance imaging (MRI) vascular origin have increased the risk of dementia [85]. In a rat experiment, the mitochondrial ribosomal protein 18 (MRPL18) gene has been related with WMH [86]. As described above, ribosomopathy including the mitochondrial functions is implicated in AD [67]. Since in METS analysis, MRPL18 was reduced by increasing of miR-532-5p, mitochondrial ribosomopathies with oxidative stress could be implicated in AD. MIRAI analysis showed that an AUC of AD USA & Germany was 1.0 (accuracy, 0.93; precision, 1.0; recall, 0.93; F value, 0.96) (Figure 4).

In AD conventional data from meta-analysis, ARNTL up regulation was observed by down regulation of miR-142-3p along with miR-206 (data not shown), which was similar case to the up regulation for the CLOCK/ARNTL axis in MCI as described. Although ARNTL gene rs2278749 and CLOCK gene rs1554483 polymorphisms have been susceptible to AD in a Chinese population, circadian rhythm gene polymorphisms including CLOCK, Period circadian regulator 2 (PER2), PER3 and hypocretin receptor 2 (OX2R) genes were not associated with AD in a Brazilian population [87-89]. It suggests that the inheritable genetic factor of circadian rhythm genes is not the basic cause of AD. On the contrary, rs2526377 (A>G) at the 17q22 locus annotated to MIR124 and BZRAP1-AS long non-coding RNAs (lncRNAs) was significantly associated with a reduced risk of AD and decreased the expression of miR-142-3p [90].

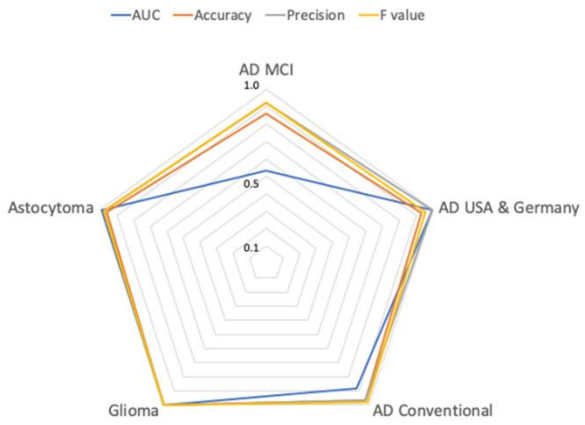

Figure 4: *Validation of METS analysis with MIRAI. METS analysis in AD and brain cancers were validated by MIRAI. An AUC (blue line), accuracy (amber line), precision (gray line) and F value (yellow line) were calculated and presented with radar charts.*

Therefore, reduced levels of miR-142-3p would be implicated in the AD risk. Further, although alpha rhythm during wake is known to be down regulated in early AD, it has been implicated in suppression of hyperpolarization activated cyclic nucleotide gated potassium channel (HCN) [91]. HCN3 was reduced by up regulation of miR-34a/c-5p with miR-449a and miR-449b-5p (data not shown). Since reduction of HCN and accumulation of Aβ have been correlated in AD, down regulation of HCN3 would be related with AD. Vesicle associated membrane protein 2 (VAMP2) was inhibited by up regulation of miR-34a/c-5p with miR-373-3p, miR-372-3p and miR-520d-3p (data not shown) [92]. VAMP2 is a component of the protein complex with the 25-kd synaptosomal-associated protein (SNAP25) and syntaxin 3 (STX3) involved in the docking and fusion of synaptic vesicles on the presynaptic membrane. VAMP2 has showed decreasing expression in aging and AD [93]. Thus, VAMP2 down regulation would be implicated in AD. These results indicate that dysregulation of circadian rhythm-dependent sleep/wake might be a common hallmark of aging including MCI and AD. NOTCH is highly expressed in the hippocampus of the human brain and plays an important role for learning and memory; therefore, reduction of NOTCH signalling is deeply involved into AD [94]. While NOTCH, human brain memory-associated protein has already been documented in previous our book, NOTCH2 was reduced by up regulation of miR-34a-5p (data not shown). So, it suggests that suppression of NOTCH2 by miR-34a-5p might be associated with both AD and brain memory. Simultaneously, miR-34a-5p up regulation inhibited MDM4 expression. MDM4 regulator of P53 (MDM4) has pro-survival role for neurons; therefore, MDM degradation is associated with neuronal death. Progressive loss of MDM4 has been shown to be a cause of Aβ-induced neural cell death during AD progression [95]. Further, anti-apoptotic protein, BCL2 was down regulated by up regulation of miR-34a/c-5p. Aβ protein down regulated BCL2 in human neuron [96]. High mobility group AT-hook 1 (HMGA1) levels were increased in brain tissues from sporadic AD [97]. HMGA1 increasing was also found in our simulation by down regulation of miR-142-3p with let-7b-5p (data not shown). HMGA1 may be implicated in AD. Thus, it is suggested that NOTCH2, MDM4 and BCL2 down regulation would be implicated in AD. Finally, an AUC of AD conventional was decreased to 0.87 (accuracy, 0.97; precision, 0.97; recall, 1.0; F value, 0.98) compared with that of AD USA & Germany in MIRAI (AUC, 1.0). AI analysis indicates that up regulation of a VEGFA signalling via miR-361-5p down regulation is more important one than circadian rhythm upon AD diagnosis and etiology. Increased VEGFA has been associated with an age-related eye disease, neovascular age-related macular degeneration (AMD), and pegaptanib, bevacizumab, ranibizumab and aflibercept can use for treatment of neovascular AMD as anti-VEGFA agents [98,99]. With respect to age-related disease, inflammation-related atherosclerotic peripheral vascular disease contains type 2 diabetes mellitus and its complication. Higher VEGF in exosome has been observed in diabetes and it was associated with diabetes status [100]. Further, chronically increasing VEFGA has been associated with cardiac hypertrophy [101]. Downregulation of miR-361-5p has been found in the plasma of neovascular AMD patients [102]. Additionally, serum VEGF reduction by treatment with cerebrolysin plus donepezil has improved functioning and cognition in patients with AD [103]. In integrative bioinformatics, VEGFA gene together with several other protein genes has been related with AD [104,105]. Our AI analysis shows that high levels of VEGFA are responsible for the progression of MCI to AD through angiodysplasia, even if

accumulation of Aβ and/or tau protein is associated with the effect of angiogenic changes for example [106,107]. In mouse AD model, vatalanib, tyrosine kinase inhibitor inhibits angiogenesis through inhibition of VEGFR signaling and reduced the number and area of Aβ plaques in the cortex [108]. It suggests that anti-VEGF agents and/or miR-361-5p mimicking locked nucleic acid (LNA) treatment has the potential to suppress Aβ in plaques or plasma, so it is an approach to address future challenges as a treatment of MCI or early AD. Interestingly, miR-361-3p has also been reduced in AD patients' brains and suppression of miR-361-3p induced high expression of its target BACE1 protein; therefore, miR-361-3p mimic administration inhibited Aβ plaques in the brain of mouse AD model [109]. By deep METS analysis, miR-316-3p was targeted to the BACE1 3'UTR (position, 3538-3545) and miR-316-5p was also targeted to the BACE1 3'UTR (position, 1658-1664) with context++ score at -0.12 and -0.04, respectively. In addition, miR-361-3p was weakly targeted to the VEGFA 3'UTR (position, 36-42) with context++ score at -0.08. As an lncRNA, small nucleolar RNA host gene 1 (SNHG1) has sponged miR-361-3p and miR-361-3p overexpression reversed the promotion effect of SNHG1 in vitro, that positively regulated Aβ [110]. Thus, the stem loop of miR-361 mimicking agents would be more effective than miR-361-5p alone. Even with the FDA's approval of the expensive aducanumab, which costs at $56000/person/year, clinical trials of large number of anti-AD drug candidates with Aβ suppression statistically failed to show effective benefits [18]. It will not be sustainable medical care for MCI and AD, even for low-income and perhaps high-income countries. Currently, one of the strongest proofs of the mRNA vaccines against the COVID-19 pandemic is the ability of nucleic acid agents, quickly delivery and cheaper, more abundant and effective worldwide. Therefore, miR-361 stem loop mimic, as an anti-VEGF nucleic acid agent may be an effective and sustainable tool for the prevention and treatment of increasing MCI or early AD incidents.

The relation between AD, MCI and brain cancer

Taken together, given the hub miRNAs in the brain cancer and AD, there was no common miRNAs from MMPs among disease. As shown in Table 2, hub miRNAs of AD MCI, AD USA & Germany, AD conventional, glioma and astrocytoma are miR-483-5p (up) and miR-142-3p (down), miR-532-5p (up) and miR-361-5p (down), miR-34a-5p (up) and miR-142-3p (down), miR-16-5p (down) and miR-497-5p (down), and miR-106a-5p (up) and miR-20a-5p (up), respectively. DNSs of hub miRNAs in AD MCI, AD USA & Germany, AD conventional, glioma and astrocytoma were 55, 35, 40, 36 and 49, respectively. As DNSs of AD USA & Germany, AD conventional and MCI were 35, 40 and 55 at the AI validated value as an AUC of 1.0, 0.87 and 0.53, respectively, and the lower quantum energy levels among two miRNAs as DNS would increase the risk of AD. However, the inverse relationship of miRNA expression levels between the brain cancer and AD was not observed in our METS analysis. Although AUC values of MIRAI in the brain cancers was statistically significance, the miRNA prediction value for MCI was not statistically enough to extract AD pathology; therefore, the MCI stage at this time MMP may be still reversible to normal condition. On the other hand, the MCI data will be some limitation via the small open data because only two miRNA panels of MCI were used in this study. So, to confirm AD prediction from MCI using the current data, much more VEGFA data in MCI should be necessary. Further clinical data was needed to in silico our simulation for building up sustainable healthcare.

Conclusion

Since the hub miRNAs were found in brain cancer and AD, there were no common miRNAs from MMPs among disease, see Table 2.

Table 2: *Summary of major hub miRNAs and their targets in AD and the brain tumors.*

Data source		Hub miRNA	Level	Target	Function	Level	DNS	AI (AUC)
Brain tumor	Glioma	miR-16-5p	down	HMGA1	Metastatic progression	up	36	1.00
		miR-497-5p	down	BCL2	Anti-apoptosis	up		
	Astrocytoma	miR-106a-5p	up	RB1	Tumor suppression	down	49	0.99
		miR-20a-5p	up	CDKN1A	Cyclin inhibition	down		
AD	MCI	miR-483-5p	up	ROCK2	RhoA/ROCK2 pathway	down	55	0.53
				RP31	Ribosomopathy	down		
		miR-142-3p.1	down	ARNTL	Circadian rhythm	up		
	US & Germany	miR-532-5p	up	MRPL18	Ribosomopathy	down	35	1.00

		miR-361-5p	down	VEGFA	VEGFA pathway	up		
	Conventional	miR-34a-5p	up	NOTCH2	Brain memory	down	40	0.87
				MDM4	Neural cell alive	down		
				BCL2	Anti-apoptosis	down		
		miR-142-3p.1	down	ARNTL	Circadian rhythm	up		

Thus, miRNA biomarkers for brain cancer, MCI and AD could be available for pathophysiologic diagnosis and prediction. It is mathematically calculated that the USA model requires approximate $8 trillion in medical and care expenses for an early and accurate diagnosis of AD; therefore, cost issues are an urgent one for establishing sustainable health management in AD. For brain cancer, early diagnosis of AD and MCI, cheaper and simpler diagnostic tools need to be developed. METS using MIRAI was used for etiologic analysis of data from the serum/plasma miRNA panel of patients with AD and cancers. Consequently, it was found that the enhancement of VEGFA via miR-361-5p down regulation is the most important cause of AD (Figure 5).

Up regulation of the circadian rhythm-related protein, aryl hydrocarbon receptor nuclear translocator like (ARNTL) via miR-142-3p down regulation was the basic pathogenicity of MCI and AD. The causative factors directly associated with Aβ were not outcome; however, in deep METS analysis, miR-361-5p and miR-361-3p were targeted to BACE1 3'UTR. Our findings upon the cause of MCI-to-AD progression through angiodysplasia could contribute to the establishment of baseline references in the diagnosis, prognosis and treatment of aging diseases in the human brain. Further, analysis of hub miRNA/target proteins in glioma and astrocytoma showed up regulation of HMGA1 by miR-16-5p down regulation, up regulation of BCL2 by miR-497-5p down regulation, and down regulation of RB1 by miR-106a-5p up regulation and down regulation of CDKN1A by miR-20a-5p up regulation, respectively; therefore, no inverse correlation of common miRNA and hub miRNA levels was observed, and there was no relationship between AD and the cause of brain cancer.

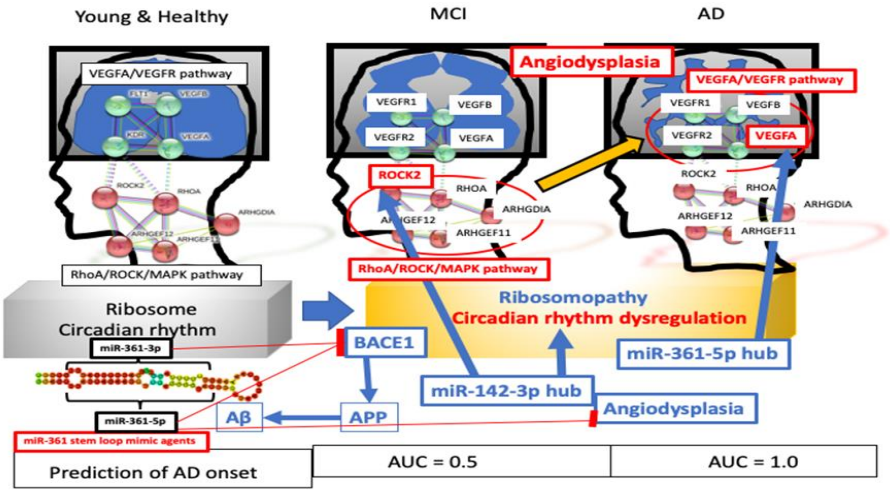

Figure 5: *Etiologic causes from MCI and AD onset. Molecular mechanisms in progression of MCI and AD were depicted in the middle panel and the left panel, respectively. Upregulated proteins and pathways were in red, downregulated ones were in blue. miR-361 stem loop mimic agents could block both angiodysplasia and Aβ accumulation in MCI and AD according to prediction of AD onset (AUC from 0.5 in MCI to 1.0 in AD).*

Thus, AD, MCI, glioma and astrocytoma can be completely differentially diagnosed by circulating miRNA biomarkers. There is one of the strongest proofs that nucleic acid agents, such as the mRNA vaccines against the COVID-19 pandemic has the ability of cheaper, more abundant and effective worldwide. Since miR-361-3p and -5p were targeted to the BACE1 3'UTR, anti-VEGFA agents and/or miR-361 stem loop mimicking locked nucleic acid (LNA) treatment may help sustainable approaches to prevent progression from MCI or early AD to AD or late AD.

Conflicts of Interest

The authors declare that there are no conflicts of interest.

References

1. Ostrom QT, Bauchet L, Davis FG, Deltour I, Fisher JL, Langer CE, et al. The epidemiology of glioma in adluts: a state of the science review. Neuro Oncol. 2014; 16: 896-913.

2. Louis DN, Perry A, Reifenberger, G, Deimling A, Branger DF, Cavenee WK, et al. The 2016 world health organization classification of tumors of the central nervous system: a summary. Acta Neuropathol. 2016; 131: 803-820.
3. Huang J, Chaudhary R, Cohen AL, Fink K, Goldlust S, Boockvar J, et al. A multicenter phase II study of temozolomide plus disulfiram and copper for recurrent temozolomide-resistant glioblastoma. J Neurooncol. 2018; 142: 537-544.
4. Stupp R, Mason WP, Bent MJ, Weller M, Fisher B, Taphoom MJ, et al. Radiotherapy plus concomitant and adjuvant temozolomide for glioblastoma. N Engl J Med. 2005; 352: 987-996.
5. Wortmann M. Importance of national plans for Alzheimer's disease and dementia. Alzheimer's Res Ther. 2013; 4: 40.
6. Masters CL, Bateman R, Blennow K, Rowe CC, Sperling RA, Cummings JI, et al. Alzheimer's disease. Nat Rev Dis Primers. 2015; 1: 15056.
7. Zhang J, Sun P, Zhou C, Zhang X, Ma F, Xu Y, et al. Regulatory microRNAs and vascular cognitive impairment and dementia. CNS Neurosci Ther. 2020; 26: 1207-1218.
8. Naik B, Mehta A, Shah M. Denouements of machine learning and multimodal diagnostic classification of Alzheimer's disease. Vis Comp Idust Biomed Art. 2020; 3: 26.
9. Zhou Q, Goryawala M, Cabreizo M, Wang J, Barker W, Loewenstein DA, et al. An optimal decisional space for the classification of Alzheimer's disease and mild cognitive impairment. IEEE Trans Biomed Eng. 2014; 61: 2245-2253.
10. Alzheimer's disease facts and figures. Alzheimers Dem. 2018; 14: 367-429.
11. Shen Y, Ye B, Chen P, Wang Q, Fan C, Shu Y, et al. Cognitive decline, dementia, Alzheimer's disease and presbycusis: examination of the possible molecular mechanism. Front Neurosci. 2018; 12: 394.
12. Zhang YW, Thompson R, Zhang H, Xu H. APP processing in Alzheimer's disease. Mol Brain. 2011; 4: 3.
13. Baek MS, Cho H, Lee HS, Lee JH, Ryu YH, Lyoo CH, et al. Effect of APOE ε4 genotype on amyloid- Aβ and tau accumulation in Alzheimer's disease. Alzheimer's Res Ther. 2020; 12: 140.
14. Tan MS, Yang YX, Wang HF, Xu W, Tan CC, Zuo CT, et al. PET amyloid and tau status are differently affected by patient features. Alzheimer's Dis. 2020; 78: 1129-1136.
15. Shen XN, Li JQ, Wang HF, Li HQ, Huang YY, Yang YX, et al. Plasma amyloid, tau, and neurodegeneration biomarker profiles predict Alzheimer's disease pathology and clinical progression in older adults without dementia. Alzheimers Dement. 2020; 12: 12104.
16. Crane PK, Trittschuh E, Mukherjee S, Saykin AJ, Sanders RE, Larson EB, et al. Incidence of cognitively defined late-onset Alzheimer's dementia subgroup from a prospective cohort study. Alzheimers Dement. 2017; 13: 1307-1316.
17. Fleck LM. Alzheimer's and aducanumab: unjust profits and false hopes. Hastings Cent Rep. 2021; 5: 9-11.
18. Walsh S, Merrick R, Milne R, Brayne C. Aducanumab for Alzheimer's disease. BMJ. 2021; 374: 1682.
19. Lundebjerg NE. My head just exploded, now what. J Am Geriatr Soc. 2021; 1-3.
20. Imbimbo BP, Ippati S, Wang M. Should drug discovery scientists still embrace the amyloid hypothesis for Alzheimer's disease or should they be looking elsewhere. Expert Opin Drug Discov. 2020; 15: 1241-1251.
21. Ding Q, Markesbery WR, Chen Q, Li F, Keller JN. Ribosome dysfunction is an early event in Alzheimer's disease. J Neurosci. 2005; 25: 9171-9175.
22. Pietrzak M, Rempala G, Nelson PT, Zheng JJ, Hetman M. Epigenetic silencing of nucleolar rRNA genes in Alzheimer's disease. PLoS One. 2011; 6: 22585.
23. Chiarini A, Whitfield J, Bonafini C, Chakravarthy B, Armato L, Pr ID, et al. Amyloid-β(25-35), an amyloid-β(1-42) surrogate, and proinflammatory cytokines stimulate VEGF-A secretion by cultured, early passage, normoxic adult human cerebral astrocytes. J Alzheimers Dis. 2010; 21: 915-926.
24. Tarkowski E, Issa R, Sjogren M, Wallin A, Blennow K, Tarkowski A, et al. Increased intrathecal levels of the angiogenic factors VEGF and TGF-beta in Alzheimer's disease and vascular dementia. Neurobiol Aging. 2002; 23: 237-243.
25. Miners JS, Palmer JC, Love S. Pathophysiology of hypoperfusion of the precuneus in early Alzheimer's disease. Brain Pathol. 2016; 26: 533-541.
26. Mahoney ER, Dumitrescu L, Moore AM, Cambronero FE, Jager PL, Koran MEI, et al. Brain expression of the vascular endothelial growth factor gene family in cognitive aging and Alzheimer's disease. Mol Psychiatry. 2019; 26: 888-896.
27. Cho SJ, Park MH, Han C, Yoon K, Koh YH. VEGFR2 alteration in Alzheimer's disease. Sci Rep. 2017; 7: 17713.
28. Fujii YR. The microRNA 2000: from HIV-1 to healthcare. Scientific Research Publishing, Inc. Irvine, CA, USA. 2017.
29. Rapp JH, Rainone S, Hebert SS. MicroRNAs underlying memory deficits in neurodegenerative disorder. Prog Neuropsychopharmacol Biol Psychiatry. 2017; 73: 79-86.
30. Brennan S, Keon M, Liu B, Su Z, Saksena NK. Panoramic visualization of circulating microRNAs across neurodegenerative diseases in humans. Mol Neurobiol. 2019; 56: 7380-7407.

31. Ham S, Kim TK, Ryu J, Kim YS, Tang YP, Im HI, et al. Comprehensive microRNAome analysis of the relationship between Alzheimer disease and cancer in PSEN double-knockout mice. Int Neurourol J. 2018; 22: 237-245.
32. Candido S, Lupo G, Pennisi M, Basile MS, Anfuso CD, Petralia MC, et al. The analysis of miRNA expression profiling datasets reveals inverse microRNA patterns in glioblastoma and Alzheimer's disease. Oncol Rep. 2019; 42: 911-922.
33. Nagaraj S, Zoltowska KM, Kaszub K, Wojda U. microRNA diagnostic panel for Alzheimer's disease and epigenetic trade-off between neurodegeneration and cancer. Aging Res Reviews. 2019; 49: 125-143.
34. Satoh JI, Kino Y, Niida S. MicroRNA-seq data analysis pipeline to identify blood biomarkers for Alzheimer's disease from public data. Biomark Insights. 2015; 10: 21-31.
35. Tan L, Yu JT, Tan MS, Liu QY, Wang HF, Zhang W, et al. Genome-wide serum microRNA expression profiling identifies serum biomarkers for Alzheimer's disease. J Alzheimers Dis. 2014; 40: 1017-1027.
36. Kopkova A, Sana J, Machackova T, Vecera M, Radova L, Trachtova K, et al. Cerebrospinal fluid microRNA signatures as diagnostic biomarkers in brain tumors. Cancers. 2019; 11: 1546.
37. Dong X, Zheng D, Nao J. Circulating exosome microRNAs as diagnostic biomarkers of dementia. Front. Aging Neurosci. 2020; 12: 580199.
38. Fujii YR. The quantum microRNA immunity in human virus-associated diseases: virtual reality of HBV, HCV and HIV-1 infection, and hepatocellular carcinogenesis with AI machine learning. Arch Clin Biomed Res. 2020; 4: 89-129.
39. Fujii YR. Quantum language of microRNA: application for new cancer therapeutic targets. Methods Mol Biol. 2018; 1733: 145-157.
40. Fujii YR. The quantum language of the microRNA gene and anti-cancer: with a dynamic computer simulation of human breast cancer drug resistance. Integr Mol Med. 2018; 5: 1-13.
41. Fujii YR. Cancer simulation from stage minus one by quantum microRNA language: lung, colorectal and pancreatic cancers. Med One. 2019; 4: 190023.
42. Fujii YR. Quantum microRNA network analysis in gastric and esophageal cancers: xenotropic plant microRNAs cure from cancerous paradox via Helicobacter pylori infection. Gastroenterol. Hepatol Endosc. 2019; 4: 1-18.
43. Fujii YR. The etiology of COVID-19 in silico by SARS-Cov-2 infection with the quantum microrna language-AI. Virol Immunol J. 2020; 4: 243.
44. Fujii YR. The COVID-19 deadly risk assessment upon the updated etiologic computer simulation by quantum microRNA language in SARS-CoV-2 infection in eo. Int J Clin Case stud Rep. 2020; 3: 142-154.
45. Fujii YR. In silico study by quantum microRNA language for development of anti-COVID-19 agents: COVID-19 is prevented by rice MiR2097-5p through suppression of SARS-Cov-2 viral microRNAs plus HIPK2 target proteins. Virol Immunol J. 2020; 4: 256.
46. Fujii YR. Quantum microRNA assessment of COVID-19 RNA vaccine: hidden potency of BNT162b2 SARS-CoV-2 spike RNA as microRNA vaccine. Adv Case Stud. 2021; 3.
47. Zhao Y, Jaber V, Alexandrov PN, Vergallo A, Lista S, Hampel H, et al. microRNA-based biomarkers in Alzheimer's disease. Front Neurosci. 2020; 14: 585432.
48. Fujii YR. The RNA gene information: retroelement-microRNA entangling as the RNA quantum code. Methods Mol Biol. 2013; 936: 47-67.
49. Huang S, Ali ND, Zhong L, Shi J. MicroRNAs as biomarkers for human glioblastoma: progress and potential. Acta Pharmacol Sinica. 2018; 39: 1405-1413.
50. Bark JM, Kulasinghe A, Chua B, Day BW, Punyadeera C. Circulating biomarkers in patients with glioblastoma. Brit J Cancer. 2020; 122: 295-305.
51. Urso PI, Urso OF, Gianfreda CD, Mezzolla V, Storelli C, Marsigliante S, et al. miR-15b and miR-21 as circulating biomarkers for diagnosis of glioma. Curr Genom. 2015; 16: 304-311.
52. Regazzo G, Terrenato I, Spagnuolo M, Carosi M, Cognetti G, Cicchillitti L, et al. A restricted signature of serum miRNAs distinguishes glioblastoma from lower grade glioma. J Exp Clin Cancer Res. 2016; 35: 124.
53. Santangelo A, Imbruce P, Gardenghi B, Belli L, Agushi R, Tamanini A, et al. A microRNA signature from serum exosomes of patients with glioma as complementary diagnostic biomarker. J Neurooncol. 2018; 136: 51-62.
54. Pang B, Fan H, Zhang IY, Liu B, Feng B, Meng L, et al. HMGA1 expression in human gliomas and its correlation with tumor proliferation, invasion and angiogenesis. J Neurooncol. 2012; 106: 543-549.
55. Liu J, Yang J, Yu L, Rao C, Wang Q, Sun C, et al. miR-361-5p inhibits glioma migration and invasion by targeting SND1. Onco Targets Ther. 2018; 11: 5239-5252.
56. Yang TQ, Lu XJ, Wu TF, Ding DD, Zhao ZH, Chen GL, et al. MicroRNA-16 inhibits glioma cell growth and invasion through suppression of BCL2 and the nuclear factor-kB1/MMP9 signaling pathway. Cancer Sci. 2014; 105: 265-271.
57. Chen XJ, Wu MY, Li DH, You J. Apigenin inhibits glioma cell growth through promoting microRNA-16 and suppression of BCL-2 and nuclear factor-kB/MMP-9. Mol Med Rep. 2016; 14: 2352-2358.

58. Wei C, Luo Q, Sun X, Li D, Song H, Li X, et al. microRNA-497 induces cell apoptosis by negatively regulating Bcl-2 protein expression at the posttranscriptional level in human breast cancer. Int J Clin Exp Pathol. 2015; 8: 7729-7739.
59. Zhi F, Shao N, Wang R, Deng D, Xue L, Wang Q, et al. Identification of 9 serum microRNAs as potential noninvasive biomarkers of human astrocytoma. Neuro-Oncol. 2015; 17: 383-391.
60. Gruszka R, Zakrzewski K, Liberski PP, Zakrzewska M. mRNA and miRNA expression analyses of the MYC/E2F/miR-17-92 network in the most common pediatric brain cancer. Int J Mol Sci. 2021; 22: 543.
61. Wang Z, Wang B, Shi Y, Xu C, Xiao HL, Ma LN, et al. Oncogenic miR-20a and miR-106a enhance the invasiveness of human glioma stem cells by directly targeting TIMP-2. Oncogene. 2015; 34: 1407-1419.
62. Nagaraj S, Kaszub KL, Debski KJ, Wojsiat J, Dabrowski M, Gabryelewicz T, et al. Profile of 6 microRNA in blood plasma distinguish early stage Alzheimer's disease patients from non-demented subjects. Oncotarget. 2017; 8: 16122-16143.
63. Ludwig N, Fehlmann T, Kern F, Gogol M, Maetzler W, Deutscher S, et al. Machine learning to detect Alzheimer's disease from circulating non-coding RNAs. Genom Prot Bioinf. 2019; 17: 430-440.
64. Kumar P, Dezso Z, MacKenzie C, Oestreicher J, Agoulnik S, Byrne M, et al. Circulating miRNA biomarkers for Alzheimer's disease. PLoS One. 2013; 8: 69807.
65. Bhatnagar S, Chertkow H, Schipper HM, Yuan Z, Shetty V, Jenkins S, et al. Increasing microRNA-34c abundance in Alzheimer's disease circulating blood plasma. Front Mol Neuro. 2014; 7: 2.
66. Catana CS, Crisan CA, Opre D, Neagoe IB. Diagnostic and prognostic value of microRNAs for Alzheimer's disease: a comprehensive meta-analysis. Med Pharm Rep. 2020; 93: 53-61.
67. Luo H, Han G, Wang J, Zeng F, Li Y, Shao S, et al. Common aging signature in the peripheral blood of vascular dementia and Alzheimer's disease. Mol Neurobiol. 2016; 53: 3596-3605.
68. Danilova N, Gazda HT. Ribosomopathies: how a common root can cuase a tree of pathologies. Dis Models Mechanisms. 2015; 8: 1013-1026.
69. Yoshikawa M, Fujii YR. Human ribosomal RNA-derived resident microRNAs as the transmitter of information upon the cytoplasmic cancer stress. Biomed Res Int. 2016; 7562085.
70. Kampen KR, Sulima SO, Vereecke S, De Keersmaecker K. Hallmarks of ribosomopathies. Nucleic Acids Res. 2020; 48: 1013-1028.
71. Thome J, Coogan AN, Woods AG, Darie CC, Habler F. CLOCK genes and circadian rhythmicity in Alzheimer Disease. J Aging Res. 2011; 2011: 383091.
72. Phan TX, Malkani RG. Sleep and circadian rhythm disruption and stress intersect in Alzheimer's disease. Neurobiol Stress. 2019; 10: 100133.
73. Kress GJ, Liao F, Dimitry J, Cedeno MR, FitzGerald GA, Holtzman DM, et al. Regulation of amyloid- β dynamics and pathology by the circadian clock. J Exp Med. 2018; 215: 1059-1068.
74. Yoo ID, Park MW, Cha HW, Yoon S, Boonpraman N, Yi SS, et al. Elevated CLOCK and BMAL1 contribute to the impairment of aerobic glycosis from astrocytes in Alzheimer's disease. Int J Mol Sci. 2020; 21: 7862.
75. Duff K, Horn KP, Foster NL, Hoffman JM. Short-term practice effects and brain hypometabolism: preliminary data from an FDG PET study. Arch Clin Neuropsychol. 2015; 30: 264-270.
76. Kinoshita C, Okamoto Y, Aoyama K, Nakaki T. MicroRNA: a key player for the interplay of circadian rhythm abnormalities, sleep disorders and neurodegenerative diseases. Clocks Sleep. 2020; 2: 282-307.
77. Rawal HA, Alghadir AH, Gabr SA. Molecular changes in circulating microRNAs' expression and oxidative stress in adults with mild cognitive impairment: a biochemical and molecular study. Clin Interv Aging. 2021; 16: 57-70.
78. Kroll J, Epting D, Kern K, Dietz CT, Feng Y, Hammes HP, et al. Inhibition of Rho-dependent kinase ROCK I/II activates VEGF-driven retinal neovascularization and sprouting angiogenesis. Am J Physiol Heart Circ Physiol. 2009; 296: 893-899.
79. Kowanetz M, Ferrara N. Vascular endothelial growth factor signaling pathways: therapeutic perspective. Mol Pathways. 2006; 12: 5018-5022.
80. Sheinerman KS, Tsivinsky VG, Abdullah L, Crawford F, Umansky SR. Plasma microRNA biomarkers for detection of mild cognitive impairment: biomarker validation study. Aging. 2013; 5: 925-938.
81. Lipnik K, Naschberger E, Laurent N, Kodajova P, Petznek H. Interferon gamma-induced human guanylate binding protein 1 inhibits mammary tumor growth in mice. Mol Med. 2010; 16: 177-187.
82. Mateo I, Llorca J, Infante J, Rodriguez E, Quintana C, Juan P, et al. Case-control study of vascular endothelial growth factor (VEGF) genetic variability in Alzheimer's disease. Neurosci Lett. 2006; 401: 171-173.
83. Zhang S, Zhau HE, Osunkoya AO, Iqbai S, Yang X, Fan S, et al. Vascular endothelial growth factor regulates myeloid cell leukemia-1 expression through neuropilin-1-dependent

activation of c-MET signaling in human prostate cancer cells. Mol Cancer. 2010; 9: 9.

84. Meng S, Cao J, Zhang X, Fan Y, Fang L, Wang C, et al. Downregulation of microRNA-130a contributes to endothelial progenitor cell dysfunction in diabetic patients via its target Runx3. PLoS One. 2013; 8: 68611.
85. Debette S, Schilling S, Duperron MG, Larsson SC. Clinical significance of magnetic resonance imaging markers of vascular brain injury: a systematic review and meta-analysis. JAMA Neurol. 2019; 76: 81-94.
86. Lopez LM, Hill D, Harris SE, Hernandez MV, Maniega SM, Bastin ME, et al. Genes from a translational analysis support a multifactorial nature of white matter hypertensities. Stroke. 2015; 46: 341-347.
87. Chen Q, Huang CQ, Hu XY, Li SB, Zhang XM. Functional CLOCK gene rs1554483 G/C polymorphism is associated with susceptibility to Alzheimer's disease in the Chinese population. J Inter Med Res. 2013; 41: 340-346.
88. Chen Q, Peng XD, Huang CQ, Hu XY, Zhang XM. Association between ARNTL (BMAL1) rs2278749 polymorphism T>C and susceptibility to Alzheimer's disease in a Chinese population. Genet Mol Res. 2015; 14: 18515-18522.
89. Pereira PA, Soares A, Bicalho MAC, Moraes EN, Diniz L, Paula JJ, et al. Lack of association between genetic polymorphism of circadian genes (PER2, PER3, CLOCK and OX2R) with late onset depression and Alzheimer's disease in a sample of a Brazilian population. Curr Alzheimer Res. 2016; 13: 1397-1406.
90. Ghanbari M, Munshi ST, Ma B, Lendemeijer B, Bansal S, Adams HH, et al. A functional variant in the miR-142 promoter modulating its expression and conferring risk of Alzheimer disease. Hum Mutat. 2019; 40: 2131-2145.
91. Sharma R, Nadkarni S. Biophysical basis of alpha rhythm disruption in Alzheimer's disease. E Neuro. 2020; 7: 293.
92. Saito Y, Inoue T, Zhu G, Kimura N, Okada M, Nishimura M, et al. Hyperpolarization-activated cyclic nucleotide gated channels: a potential molecular link between epileptic seizures and Aβ generation in Alzheimer's disease. Mol Neurodegene. 2012; 7: 50.
93. Berchtold NC, Coleman PD, Cribbs DH, Rogers J, Gillen DL. Synaptic genes are extensively downregulated across multiple brain regions in normal human aging and Alzheimer's disease. Neurobiol Aging. 2013; 34: 1653-1661.
94. Woo HN, Park JS, Gwon AR, Arumugam TV, Jo DG. Alzheimer's disease and Notch signaling. Biochem Biophys Res Commun. 2009; 390: 1093-1097.
95. Colacurclo DJ, Zyskind JW, Sciutto KL, Espinoza CA. Caspase-dependent degradation of MDMx/MDM4 cell cycle regulatory protein in amyloid β-induced neuronal damage. Neurosci Lett. 2015; 609: 182-188.
96. Paradis E, Douillard H, Koutroumanis M, Goodyer C. Amyloid beta peptide of Alzheimer's disease downregulates Bcl-2 and upregulates bax expression in human neurons. J Neurosci. 1996; 16: 7533-7539.
97. Manabe T, Katayama T, Sato N, Hitomi J, Yanagita T, Kudo T, et al. Induced HMGA1a expression causes aberrant splicing od Presenilin-2 pre-mRNA in sporadic Alzheimer's disease. Cell Death Different. 2003; 10: 698-708.
98. Marneros AG. Increased VEGF-A promotes multiple distinct aging disease of the eye through shared pathomechanisms. EMBO Mol Med. 2016; 8: 208-231.
99. Papadopoulos Z. Neovascular age-related macular degeneration and its association with Alzheimer's disease. Curr Aging Sci. 2020; 13: 102-112.
100. Wu SF, Hooten NN, Freeman DW, Mode NA, Zonderman AB. Extracellular vesicles in diabetes mellitus induce alterations in endothelial cell morphology and migration. Transl Med. 2020; 18: 230.
101. Marneros AG. Effects of chronically increased VEGF-A on the aging heart. FASEB J. 2018; 32: 1550-1565.
102. Grassmann F, Schoenberger PGA, Brandl C, Schick T, Hasler D. A circulating microRNA profile is associated with late-stage neovascular age-related macular degeneration. PLoS One. 2014; 9: 107461.
103. Alvarez ZA, Alvarez I, Martinez A, Romero I, Benito C, Suarez I, et al. Serum VEGFA predicts clinical improvement induced by cerebrolysin plus donepezil in patients with advanced Alzheimer's disease. Int J Neuropsychopharmaco. 2020; 23: 581-586.
104. Li Z, Xiong Z, Manor LC, Cao H, Li T. Integrative computational evaluation of genetic markers for Alzheimer's disease. Saudi J Biol Sci. 2018; 25: 996-1002.
105. Gholizadeh E, Khaleghian A, Seyfi DN, Karbalaei R. Showing NAFLD, as a key connector disease between Alzheimer's disease and diabetes via analysis of system biology. Gastroenterol Hepatol Bed Bench. 2020; 13: 89-97.
106. Vagnucci AH, Li WW. Alzheimer's disease and angiogenesis. Lancet. 2003; 361: 605-608.
107. Vergara MI, Nieves AE, Diaz R, Perinan G, Urena N, Luis C, et al. Non-productive angiogenesis disassembles Aβ plaque-associated blood vessels. Nat Commun. 2021; 12: 3098.
108. Jeon SG, Lee HJ, Park H, Han KM, Hoe HS. The VEGF inhibitor vatalanib regulates AD pathology in 5xFAD mice. Mol Brain. 2020; 13: 131.
109. Ji Y, Wang D, Zhang B, Lu H. MiR-361-3p inhibits β-amyloid accumulation and attenuates cognitive deficits

through targeting BACE1 in Alzheimer's disease. J Integr Neurosci. 2019; 18: 285-291.

110. Gao Y, Zhang N, Lv C, Li N, Li X, Li W, et al. IncRNA SNHG1 knockdown alleviates amylod- β-induced neural injury by regulating ZNF217 via sponging miR-361-3p in Alzheimer's disease. J Alzheimers Dis. 2020; 77: 85-98.